Available online at www.sciencedirect.com

SCIENCE DIRECT

Experimental Cell Research 312 (2006) 215 – 232

Experimental Cell Research

www.elsevier.com/locate/yexcr

Research Article

Growth hormone activity in mitochondria depends on GH receptor Box 1 and involves caveolar pathway targeting

Cécile Perret-Vivancos[a,1,2], Aude Abbate[a,1], Dominique Ardail[b], Mireille Raccurt[a], Yves Usson[c], Peter E. Lobie[d], Gérard Morel[a,*]

[a]CNRS UMR 5123, Bât. R. Dubois, Université Claude Bernard–Lyon 1, 43 Bd du 11 Novembre 1918, 69622 Villeurbanne cedex, France
[b]INSERM U189–Faculté de médecine Lyon Sud, 69921 Oullins cedex, France
[c]UMR 5525 CNRS, Institut de l'Ingénierie de l'Information de Santé (IN3S) Domaine de la Merci, Université Joseph Fourier, 38706 La Tronche cedex, France
[d]Liggins Institute, University of Aukland, 2-6 Park Avenue, Private Bag, Aukland 92019, New Zealand

Received 29 April 2005, revised version received 15 September 2005, accepted 14 October 2005

Abstract

Growth hormone (GH) binding to its receptor (GHR) initiates GH-dependent signal transduction and internalization pathways to generate the biological effects. The precise role and way of action of GH on mitochondrial function are not yet fully understood. We show here that GH can stimulate cellular oxygen consumption in CHO cells transfected with cDNA coding for the full-length GHR. By using different GHR cDNA constructs, we succeeded in determining the different parts of the GHR implicated in the mitochondrial response to GH. Polarography and two-photon excitation fluorescence microscopy analysis showed that the Box 1 of the GHR intracellular domain was required for an activation of the mitochondrial respiration in response to a GH exposure. However, confocal laser scanning microscopy demonstrated that cells lacking the GHR Box 1 could efficiently internalize the hormone. We demonstrated that internalization mediated either by clathrin-coated pits or by caveolae was able to regulate GH mitochondrial effect: these two pathways are both essential to obtain the GH stimulatory action on mitochondrial function. Moreover, electron microscopic and biochemical approaches allowed us to identify the caveolar pathway as essential for targeting GH and GHR to mitochondria.

Keywords: GH; GHR mutations; Mitochondrion; NADH; FAD; Respiration; Endocytosis; Caveolin-1

Introduction

The biological actions of growth hormone (GH) are initiated by its interaction with specific membrane-bound receptors present at the surface of target cells. The growth hormone receptor (GHR) belonging to the type I of cytokine receptor family is characterized by a single transmembrane domain and the lack of an intrinsic catalytic activity [1]. GH-induced tyrosine phosphorylation of GHR depends on the ability of the receptor to activate the tyrosine kinase Jak2, a member of Janus kinase family [2,3] which initiates most of GH-dependent signal transduction pathways. A proline-rich region, termed Box 1, localized between amino acids 297 and 311 of GHR intracellular domain and well-conserved within members of cytokine receptors family, is required for association of Jak2 with GHR as well as for GH-dependent activation of Jak2 [2,4]. Despite the leading role played by Box 1, the C-terminal domain of the receptor also takes part in GH-induced intracellular signaling [5,6]. Upon binding to its receptor, GH internalizes via clathrin coated pits pathway to be degraded in lysosomes [7] and via caveolae probably to be redistributed to different subcellular

Abbreviations: CHO, Chinese hamster ovary; FAD, flavin adenine dinucleotide; GHR, growth hormone receptor; hGH, human growth hormone; NADH, reduced nicotine adenine dinucleotide; rGH, rat growth hormone.

* Corresponding author. Fax: +33 4 72 43 29 27.
E-mail address: gerard.morel@univ-lyon1.fr (G. Morel).

[1] The first two authors contributed equally to this work.

[2] Current address: Centre of Electron Microscopy, University of Lausanne, rue du Bugnon 27, CH-1005 Lausanne, Switzerland.

0014-4827/$ - see front matter © 2005 Elsevier Inc. All rights reserved.
doi:10.1016/j.yexcr.2005.10.027

compartments including nucleus and mitochondria [8]. Neither deletion of Box 1 nor simultaneous mutation of the 4 prolines in this region impaired GH internalization and nuclear translocation [9]. Clathrin coated pit-dependent GHR endocytosis has been demonstrated to be regulated by the ubiquitin conjugation system [10,11]. GHR intracellular region targeted by the ubiquitin system is localized in the cytosolic tail as a 10-amino-acid-long sequence, DSWVEFIELD, termed UbE (ubiquitin-dependent endocytosis) motif [12]. In rat GHR, this motif includes a phenylalanine residue in position 346 that has been identified as being critical for ligand-mediated internalization [13], but at least some aspects of GH-dependent intracellular signaling are maintained. GHR ubiquitination, endocytosis and degradation could be independent of signal transduction via Jak2 [14]. Caveolae are thought of as a subset of membrane entities known as lipid rafts [15]. They function to organize the plasma membrane into a series of microdomains that act as platforms for conducting many cellular functions [16]. Caveolae are selectively associated with a key structural and functional membrane protein, caveolin, which is a cytoplasmic oriented integral protein [17]. Caveolae are now well accepted as structures involved not only in transcytosis but also in other processes such as cell signaling [18–20]. In effect, particularly caveolin-1 can interact with plasma membrane receptor and signaling molecules [20].

Combined intracellular mechanisms result in the biological responses among which anabolic [21,22] and lipolytic [23] effects of the hormone are well demonstrated. GH improves lipid oxidation by increasing the availability of substrates and, in some cases, by raising the cell mitochondrial activity [24]. GH action on hepatic mitochondrial function of hypophysectomized rats has been reported to activate respiration [25–27], but this remains questioned [28–30]. Moreover, GH was specifically internalized within liver [31] and pituitary [32] mitochondria in vivo as early as 2 min after an injection of radioactive GH. The detection of GH in mitochondria raises the question of its functional importance.

To elucidate the mechanism involved in the GH-induced stimulation of mitochondrial oxidative capacity and the role played by its receptor, GH effects on mitochondrial activity were analyzed by using two-photon excitation microscopy and polarography approaches. In the same time, we tracked GH internalization in liver for caveolae pathway and in CHO cell lines stably transfected with truncated, deleted or mutated forms of GHR for clathrin coated pits pathway. Our results show that GH acts on mitochondrial oxidative capacity through the Box 1 region of GHR supposedly by activating NADH oxidation in mitochondria. Moreover, the two main internalization processes occurred as positive regulators: they appear to be both necessary to obtain a mitochondrial stimulation in response to GH. In addition, GH and its receptor can be targeted to mitochondria via the caveolar route.

Materials and methods

Hormone and antibodies

Rat GH (rGH) and a guinea pig anti-rGH antibody were obtained from Dr. A.F. Parlow (National Hormone and Pituitary program). Reagents for cell culture were purchased from Eurobio (Les Ulis, France). Adult male Wistar rats (250 g) were from Iffa Credo (L'Arbresle, France). Prestained molecular weight markers were obtained from BioRad (Ivry sur Seine, France). Hybond-P PVDF membrane, ECL plus Western Blotting Detection System were purchased from Amersham Biosciences Europe, GmbH (Orsay, France). Methyl-β-cyclodextrin was purchased from Sigma-Aldrich (L'Isle d'Abeau, France). The following antibodies were used in this work: a polyclonal IgG raised against rat caveolin-1 (Transduction Laboratories, Lexington, KY, USA); a polyclonal IgG raised in guinea pig against rGH was a gift from the National Hormone and Pituitary Program (NHPP, Harbour–UCLA Medical Center, Torrance, CA, USA); a monoclonal mouse antibody against GH receptor (mAb 263) was a generous gift from Dr. M.J. Waters (Queensland University, Brisbane); a goat anti-rabbit IgG horseradish peroxidase was purchased from Amersham Biosciences Europe GmbH (Orsay, France); and goat IgG coupled to gold particles were from British Biocell International (Cardiff, UK).

Cellular transfection of GH receptor cDNA

The expression plasmid, pIPB-1, containing the full-length cDNA of GHR (GHR_{1-638}), under the transcriptional control of the human metallothionein IIa promoter and the simian virus (SV) 40 enhancer was constructed as previously described [33]. cDNAs encoding GHR truncation mutants were constructed by introducing stop codons at position 295 (GHR_{1-294}) and at position 455 (GHR_{1-454}) using in vitro mutagenesis. The construction of GH receptor cDNA expression plasmids containing deletion of Box 1 ($GHR_{\Delta297-311}$) and a single point mutation in position 346 (GHR_{F346A}) has been previously described [2,13,34]. The cDNA constructions were transfected into CHO-K1 cells with lipofectin together with the pIPB-1 plasmid that contains a neomycin resistance gene fused to the thymidine kinase promoter [35]. Stable transfected cells were selected using 1 mg/ml G418, and transfectants were expressed into CHO cells that were further named CHO-GHR_{1-638}, -GHR_{1-294}, -GHR_{1-454}, -$GHR_{\Delta297-311}$ and -GHR_{F346A}.

Polarographic analysis of CHO cells respiratory activity

Exponentially growing CHO cells were incubated in serum-free HAM's F12 medium plus 50 U/ml penicillin and 50 μg/ml streptomycin for 12 h. For treatment with methyl-β-cyclodextrin to disturb caveolae formation by depleting cholesterol, serum-starved cells were incubated in the same

medium added of 3 mM methyl-β-cyclodextrin for 1 h at 37°C. The cells were then washed twice in ice-cold phosphate-buffered saline (PBS) and harvested in Tris-based, Mg^{2+}-, Ca^{2+}-deficient (TD) buffer (0.137 M NaCl/5 mM KCl/0.7 mM Na_2HPO_4/25 mM Tris–HCl, pH 7.4 at 4°C), spun and resuspended in ice-cold TD buffer after removing the supernatant [36]. The concentration of cellular proteins was quantified with Bio-Rad protein assay (500–0113; with BSA as standard) and adjusted to a final concentration of 10 mg/ml. Rates of oxygen consumption were measured with a Clarck-type oxygen electrode, model DW1 from Hansatech Instruments Laboratories (Norfolk, UK). The chamber, thermostatically controlled at 37 ± 2°C, was filled with 1.8 ml of respiratory medium (corresponding to TD buffer pH 7.4) saturated with room air. For each cell line (CHO-GHR_{1-638}, -GHR_{1-294}, -GHR_{1-454}, -$GHR_{\Delta 297-311}$ and -GHR_{F346A}), 4.5 mg cellular protein in 1.8 ml TD buffer was added to the cell and incubated for 15 min with 50, 200 or 500 nM rGH under constant stirring. Controls were performed in the same conditions for each cell line without rGH. The electrode was calibrated with demineralized water and TD buffer at 37°C based on the oxygen content of water [36].

Hormone internalization

For hormone internalization kinetics, CHO cells were grown to ~80% confluence in HAM's F12 medium supplemented with 10% fetal calf serum, 50 U/ml penicillin and 50 μg/ml streptomycin before being serum deprived for 12 h. Cells were then incubated for the indicated time periods with 50 nM rGH, washed in serum-free medium and subsequently fixed for 15 min in ice-cold 4% paraformaldehyde in PBS, pH 7.4 at the end of respective time intervals. The cells were permeabilized in 0.1% Triton X-100 in PBS for 5 min, washed extensively with PBS and incubated for 1 h with an anti-rat GH antibody diluted to 1/1000 (1 μg/ml) and an anti-rGHR (mAb 263) antibody diluted to 1/50 (25 μg/ml). GH and GHR detection was performed with Cy3™ conjugated goat anti-guinea pig IgG diluted to 1/500 and Rhodol green™ conjugated goat anti-mouse IgG (Molecular Probes, Leiden, Netherlands) diluted to 1/100, respectively. Controls were performed by (a) omission of the primary antibody, (b) replacing primary antibody with the same protein concentration of preimmune mouse or guinea pig serum and (c) preincubation (24 h at 4°C) of anti-rGH with 50 μg/ml of recombinant hGH or mAb 263 with 20 μg/ml recombinant receptor extracellular domain.

Confocal laser scanning microscopy

All images were acquired with a Zeiss Laser scanning microscope 410 confocal microscope equipped with laser sources, three separate detection channels with their own pinhole detector and a fourth detection channel for DIC (Nomarski) transmitted light scanning microscopy. The fluorescence images of Cy3 and Rhodol green were collected sequentially on two different channels to avoid cross-talk between fluorescence signals. Cy3 fluorescence was excited with a 543-nm HeNe laser source. A 560-nm dichroic beam splitter was used to separate laser excitation from emitted fluorescence, and an additional 590-nm long-pass filter was used after the pinhole in order to reject non-specific fluorescence. Rhodol green fluorescence was excited with a 488-nm Argon laser source. A 510-nm dichroic beam splitter was used to separate laser excitation from emitted fluorescence and an additional 515–545-nm band pass filter was used after the pinhole to reject non-specific fluorescence. The pinhole aperture was set to one Airy disk unit for each channel. An image of the same field was recorded in DIC transmitted light in order to facilitate the cell and nuclear contour delineation in the further image analysis stage. Image averaging (Kalman filtering) was used for the acquisition of the fluorescence images to improve the signal-versus-noise ratio.

Analysis of confocal laser scanning microscopy images

Ten image triplets (Cy3–Rhodol green–DIC) were recorded per experimental slide. The images were stored on a computer disk and analyzed with a SAMBA 2005 image analysis system (SAMBA Technologies, Meylan, France). Dedicated software was developed for this particular application. Briefly, the DIC image of a triplet was used to interactively extract the contours of the cells and of the cell nuclei. From these contours, the program built the cytoplasm and nucleus binary masks of each cell. Then the Cy3 image was loaded. For each cell, the fluorescence intensities (arbitrary unit) were measured using the previously obtained binary masks inside the cytoplasm and the nucleus. Two parameters were obtained: the integrated fluorescence, which is the sum of intensity values measured within the mask; and the average fluorescence intensity, which is the integrated fluorescence divided by the area (in pixels) of the binary mask. Next, the Rhodol green image was loaded, and the same measurements were made using the binary masks as previously described [9].

Analysis by two-photon excitation fluorescence microscopy of NADH and oxidized flavoproteins in CHO cells

Redox fluorometry was based on intrinsic fluorescence of reduced pyridine nucleotides (NADH) and oxidized flavoproteins, providing a way to determine cellular energy metabolism as a reflect of mitochondrial functioning [37–40]. Fluorescence images were collected in situ by using with near-infrared (NIR) excitation. Two-photon excitation microscopy provides advantages such as negligible out-of focus photobleaching, reduced light scattering and photodamage and improved fluorescence collection efficiency ([41], reviewed by [42–44]).

Autofluorescence of mitochondrial oxidized flavoproteins and NADH was imaged using a two-photon excitation confocal laser scanning microscopy (LSM510 NLO, Zeiss). The images were collected with a 40× water immersion lens that prevented from geometrical aberrations when observing in vitro living cells. The autofluorescence of oxidized flavoproteins was excited with the 488 nm line of an Argon laser, the laser output power was set to an average of 8 mW. The fluorescence was collected through a 510-nm dichroic beam splitter and a 505–550-nm band pass filter. The pinhole aperture was set to one Airy disk unit. The autofluorescence of NADH was imaged by two-photon excitation using a femto-second pulsed infrared laser (Tsunami+MilleniaVIII, SpectraPhysics). The pulse frequency was set at 80 MHz with a pulse width of 100 femto-second. The infrared line was tuned to 720 nm. The laser output power was set to 400 mW. The fluorescence signals were collected through a multiline beam splitter with maximum reflections at 488 ± 10 (for rejection of the 488 nm line) and above 700 nm (for rejection of infrared excitation). A second 490-nm beam splitter was used to discriminate the NADH signal from the flavoprotein signal. Then the flavoprotein signal passed through a 500–550-nm band pass filter with an additional infra-red rejection filter before being collected through a pinhole (one Airy disk unit). The NADH signal was redirected to a 390–465-nm band pass filter with an additional infrared rejection filter.

CHO cells were cultured in 2 wells cover-glass in Hams'F12 medium supplemented with 10% fetal calf serum, 50 U/ml penicillin and 50 μg/ml streptomycin and seru-starved for 12 h before rGH stimulation. During the experiment, cells could only be kept at room temperature. To monitor GH-induced fluorescence changes, one image was acquired to characterize the baseline autofluorescence intensity. Each image (512 × 512 pixels) was collected by raster scanning the focused laser beam over a typical sample area of ~197 × 296 μm. Each image was acquired in ~1 s, and the average pixel dwell time for the scanning laser beam was ~0.6 μs. Subsequently, increasing rGH concentrations were added carefully without disturbing the attached cells within the microscopic field of view. Images were acquired for specified time periods immediately after hormone addition. Both NADH and oxidized flavoproteins fluorescences of single field were sequentially integrated for the studied time period in cytoplasm and nucleus using the image analysis program SAMBA 2005 (SAMBA Technologies, Meylan, France) modified for this particular application. The average fluorescence intensity of cytoplasm was set off the nucleus background intensity to improve signal-versus-noise ratio.

Experimental animals

Thirty male pathogen-free Wistar rats, weighing 250–300 g (IFFA Credo, St Germain sur l'Arbresle, France) were housed in a temperature-controlled room (22 ± 2°C) with a 12-h light, 12-h dark cycle and were fed with water and Purina laboratory chow ad libitum. GH was administrated 10–11 h after light anesthetized.

Preparation of liver mitochondrial fraction

Rat liver mitochondria were prepared as previously described [45]. Briefly, livers were immersed in ice-cold isolation medium (250 mM sucrose, 10 mM Hepes buffer, pH 7.4, 1 mM EDTA). Mitochondria were prepared by differential centrifugations and extensively washed in isolation medium before purification. The integrity of isolated mitochondria was determined polarographically with a Clark-type oxygen electrode. The respiratory control (state 3/state 4 respiration) ratios of different liver mitochondrial preparations were in the ranges of 5.5–6.5. Crude mitochondria were purified by layering on top of 20 ml of medium containing 25 mM Hepes buffer, pH 7.4, 225 mM mannitol, 1 mM EDTA, 1% BSA and 30% Percoll. Gradients were centrifuged for 30 min at 95,000 *g* as previously reported [46], and a dense band containing purified mitochondria was then recovered from approximately 2/3 down the tube. Finally, purified mitochondria were removed from the gradient and extensively washed in the isolation medium in order to remove Percoll.

Electron microscopic preparations

Ultrathin frozen sections of rat liver

After rat decapitation, liver was quickly removed and fixed in 4% paraformaldehyde as small pieces during 2 h at room temperature. Samples were cryoprotected in 0.4 M sucrose/phosphate buffer solution for 2 h at room temperature and frozen in a cold gradient of fuming nitrogen (Biogel, CFPO, Saint Priest, France) to −6°C. Samples were then immersed in liquid nitrogen [47]. Ultrathin frozen sections of 80-nm thickness were obtained using a dry sectioning method at −120°C with an Ultracut S ultramicrotome (Leica, Vienna, Austria). All sections were mounted on 400 mesh collodion-carbon-coated nickel grids.

Liver mitochondria fraction

Purified mitochondria were incubated or not in presence of 50 nM rGH and then centrifuged at 8500 *g*. The mitochondria were washed and centrifuged 3 times in 0.1 M phosphate buffer, pH 7.4 at 4°C, and the last time, the pellet was cut into small pieces and fixed for 30 min at room temperature in 4% paraformaldehyde–0.1% glutaraldehyde in 0.1 M phosphate buffer, pH 7.4. Samples were washed 3 times 10 min in 0.1 M phosphate buffer, pH 7.4. They were then dehydrated successively by 15-min incubation with 30%, 50%, 70% and 95% alcohol. They were progressively embedded at room temperature in increasing concentration of LR-White resin (Sigma-Aldrich, St Quentin-Fallavier, France)/alcohol 95%: 3 baths of 60 min with the mixture

LR-White/alcohol (1:2, 1:1 and 2:1, respectively). Finally, they were embedded in pure resin for 90 min. Polymerization was performed in gelatin capsules at 60°C for 24 h. Ultrathin sections of 80 nm were obtained using an Ultracut S ultramicrotome (Leica, Vienna, Austria) and transferred on 200 mesh collodion-carbon-coated nickel grids.

Immunocytological reactions

For cryo-immunogold electron microscopy [8,48], localization of GH, GHR and caveolin-1 was performed using polyclonal Guinea pig anti-rGH (1/1000), monoclonal mouse mAb 263 anti-GHR (1/1000) and rabbit anti-caveolin-1 (1/400) antibodies respectively, in 0.1 M phosphate buffer, 0.3 M NaCl, 0.5% BSA, pH 7.4). They were revealed by an anti-guinea pig IgG or an anti-mouse IgG conjugated with 10-nm gold particles and with an anti-rabbit IgG conjugated with 5-nm gold particles (British Biocell International, Cardiff, UK), respectively. Immunogold reagents were used at 1/50 in 20 mM Tris, 0.3 M NaCl, 0.5% BSA, pH 8.2. Concomitantly, coimmunodetection of GH and caveolin-1 or GHR and caveolin-1 were performed. The sections were then contrasted by incubation in 3% uranyl acetate, pH 7, during 10 min, and were finally embedded into methylcellulose.

For localization of the same proteins on mitochondrial fractions embedded in LR-White resin, the same antibodies were used but at different dilutions: anti-rGH (1/500), mAb 263 (1/500) and anti-caveolin-1 (1/200). These antibodies were revealed using the same secondary antibodies as above but conjugated to 10-nm gold particles. Dilution buffers were supplemented by 0.05% Tween 20, and the sections were contrasted using 4% uranyl acetate, pH 7, for 30 min, at room temperature.

Electron micrographs were taken with a Philips CM120 electron microscope, operating at 80 kV (Centre Technologique des Microstructures, Villeurbanne, France).

Western blotting

Samples were diluted in 50 mM Tris–HCl (pH 6.8) containing 90% (vol/vol) glycerol, 0.05% bromophenol blue, 3% (wt/vol) SDS. Protein weight marker and protein concentrates were denatured at 95°C, for 5 min, in the presence of DTT. The samples were then loaded onto a discontinuous polyacrylamide gel (4% acrylamide stacking and 15% resolving gels), which was run for 1 h with a constant current of 40 mA. After SDS/PAGE, proteins were blotted onto Hybond-P membranes (Amersham Biosciences Europe, GmbH) at 4°C for 1 h using a Bio-Rad transblotting apparatus at 200 mA. The membrane was first incubated with 5% (wt/vol) fat-free milk in 50 mM Tris–HCl, 150 mM NaCl, 0.05% (wt/vol) Tween 20, pH 7.3 (TBST) at room temperature during 1 h and then with an affinity-purified polyclonal antibody raised in rabbit against rat caveolin-1 (diluted at 1:1000 in TBST with 5% (wt/vol) fat-free milk) overnight at 4°C. Afterwards, the membrane was washed four times in TBST (5 min per wash) and incubated with a goat anti-rabbit antibody coupled to horseradish peroxidase (1:10,000 in blocking solution), at room temperature, for 90 min. Finally, the membrane was washed 4 times in TBST, and the bound antibody was detected using an ECL detection system (Amersham Biosciences Europe, GmbH).

Quantitative evaluation

For quantitative evaluation of GH, GHR and caveolin-1 distribution in isolated mitochondria of rat liver, at least 50 mitochondria of each experiment (10 min GH-stimulated and non-stimulated mitochondria) were analyzed for each antibody used. The electron micrographs were scanned, and the surfaces of the mitochondria were determined using the NIH Image 1.58 software (Research Service Branch). The number of individual gold particles (10 nm in diameter) was counted by hand, and the labeling density was expressed as the number of gold particle per micrometer squared.

Statistics

All data are expressed as mean ± SEM. Data from two-photon excitation were analyzed using the ANOVA and subsequently by a pair-wise test, all the others by a pair-wise test. Results were considered significant at the 5% level.

Results

In order to demonstrate the importance of the intracellular routing of internalized GH in cellular respiration, we first determined by polarographic analysis the optimal concentration of GH to obtain the maximal oxygen consumption in CHO cells stably transfected with the complete rat GHR cDNA (CHO-GHR_{1-638}). A stimulation of oxygen consumption was observed in response to rGH exposure (Fig. 1A), allowing us to determine 200 nM as the optimum concentration to obtain a maximal stimulation of oxygen consumption. With 50 nM concentration of rGH, oxygen consumption increased progressively between 2 and 15 min (40% stimulation), while the final concentration of 200 nM rGH induced a maximal metabolic activity (60% stimulation compared to control without GH) within 10 min (Fig. 1A). Inversely, no change was observed with an exposure to 500 nM rGH, corresponding to the saturation effect of a non physiological dose. Similarly, a saturation phase was observed with 200 nM after 10 min. Incubation of 200 nM rGH in CHO cells expressing the full-length GHR (CHO-GHR_{1-638}) and the C-terminally truncated GHR (CHO-GHR_{1-454}) shows a significant increase of oxygen

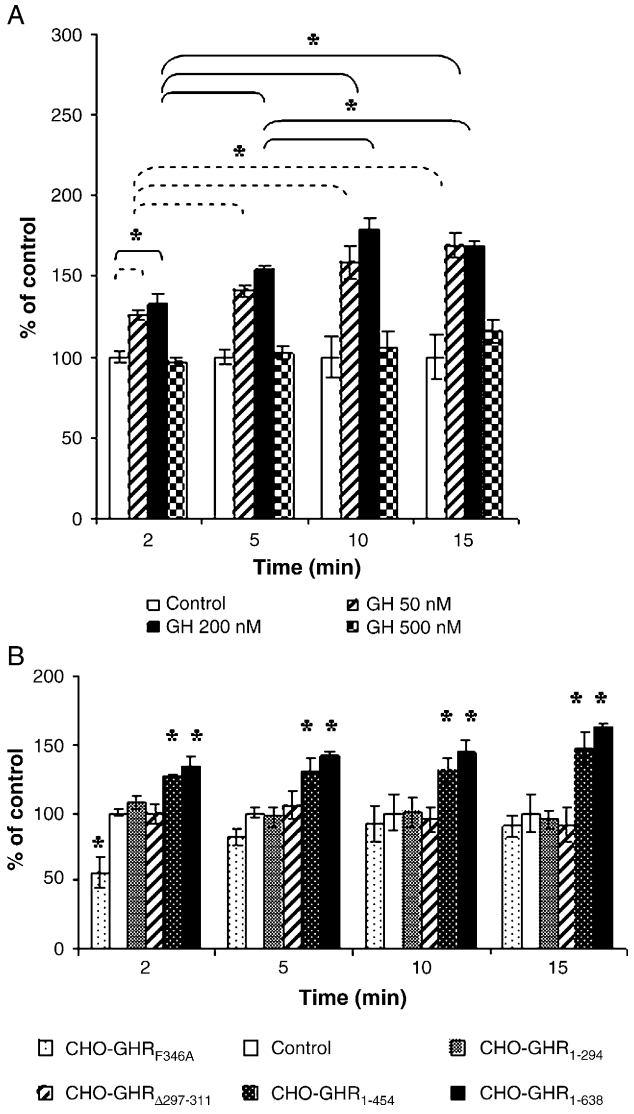

Fig. 1. Respiration of CHO cells using polarographic analysis. (A) The oxygen consumption of CHO-GHR$_{1-638}$ cells was analyzed as a reference after 15 min of 0, 50, 200 and 500 nM GH incubation as described in Materials and methods. Control is corresponding to polarographic analysis performed on CHO-GHR$_{1-638}$ without GH stimulation. The results are expressed as the mean of 3 experiments ± SEM and are normalized as a percentage of those obtained with the controls. Results were considered significant (*) at the 5% level. - - - - - Compares control to 50 nM GH incubation; —— compares control to 200 nM GH incubation. (B) The oxygen consumption of CHO cells expressing the GHR deleted of intracellular domain (CHO-GHR$_{1-294}$), the full-length GHR (CHO-GHR$_{1-638}$), the C-terminally truncated GHR (CHO-GHR$_{1-454}$), the GHR lacking the Box 1 region (CHO GHR$_{\Delta297-311}$) and the GHR construct with a point mutation of phenylalanine 346 (CHO GHR$_{F346A}$). 200 nM rGH was used for the incubation of all the cell types with the hormone, and oxygen consumption was analyzed in the same conditions as in Fig. 1. The results are expressed as the mean of 3 experiments ± SEM and are normalized as a percentage of those obtained with the controls. The results were considered significant (*) at the 5% level.

consumption studied by polarographic analysis for all times studied (Fig. 1B). Inversely, the GHR construct with a point mutation of phenylalanine 346 (CHO-GHR$_{F346A}$) presents a significant decrease in cellular respiration comparing to control at 2 min (Fig. 1B). The others cell populations did not show any significant difference at all times studied.

To determine what region of the GHR could have an effect on mitochondrial function and internalization processes after a GH stimulation, confocal laser scanning microscopy, two-photon excitation fluorescence microscopy and polarographic analysis were performed on different kinds of cells expressing different forms of GHR.

The intracellular GHR-region is required to obtain a GH-positive effect on cellular respiration and internalization processes.

Furthermore, we wanted to verify this functional short term effect of GH on mitochondrial function in CHO-GHR$_{1-638}$ cells. To do so, mitochondrial NADH oxidation and oxidized flavoproteins reduction, reflecting activation of mitochondrial respiratory chain, were examined in these cells using two-photon excitation microscopy. Fig. 2 illustrates the autofluorescence emitted by NADH (in blue) and oxidized flavoproteins (in green) in CHO-GHR$_{1-638}$ cells exposed for 30 min to 200 nM rGH. Poor superposition of the 2 autofluorescence distributions was observed. NADH, and oxidized flavoproteins seem to localize in different mitochondria. The NADH signal was homogeneously distributed in the perinuclear area rather extended from the nucleus, while oxidized flavoproteins fluorescence was mainly concentrated in large bright congregates randomly localized in the cytoplasm. The incubation of CHO-GHR$_{1-638}$ with 200 nM rGH during 30 min resulted in a decrease of NADH signal intensity (Fig. 3A) as early as 2 min and became significant from 5 min ($P < 0.05$) compared to control (Fig. 4A). Signal

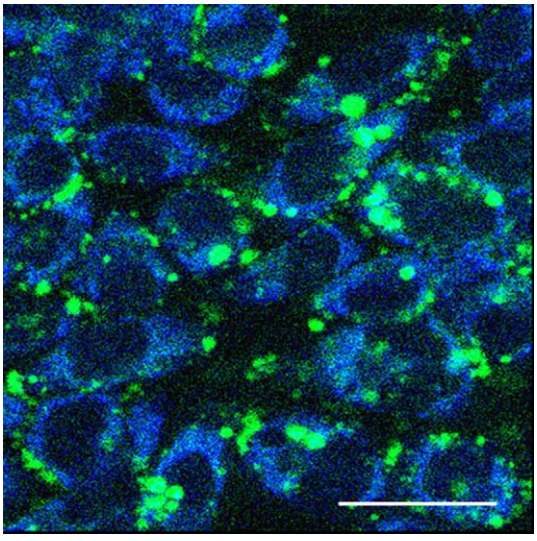

Fig. 2. Dual localization of intrinsic fluorescence of reduced pyridine nucleotides (NADH) visualized in blue with two-photon excitation confocal laser scanning microscopy and oxidized flavoproteins visualized in green with one-photon excitation confocal laser scanning microscopy in CHO cells expressing the full-length GHR (GHR$_{1-638}$) treated for 30 min to 200 nM rGH. Magnification bar is 30 μm.

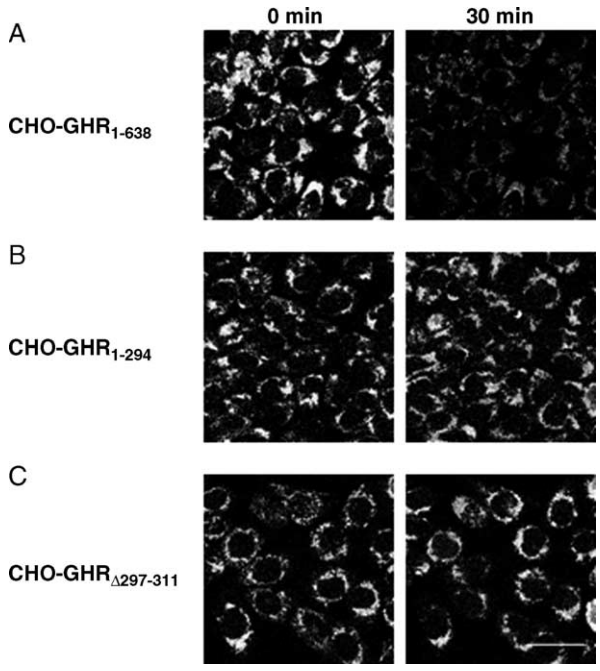

Fig. 3. Effect of 30-min exposure to 200 nM rGH on NADH autofluorescence in CHO cells expressing the full-length GHR (CHO-GHR_{1-638}) (A), the GHR deleted of intracellular domain (CHO-GHR_{1-294}) (B), and in CHO cells expressing the GHR lacking the Box 1 region (CHO $GHR_{\Delta 297-311}$) (C). The intrinsic fluorescence of NADH was visualized in the left hand column for the controls and in the right hand column for GH-stimulated CHO cells by two-photon excitation confocal laser scanning microscopy. Magnification bar is 30 μm for all photographs.

intensity declined progressively until 15 min and stabilized (to −20%/control) between 15 and 30 min with 200 nM rGH (Fig. 4A). No significant difference was observed in CHO-GHR_{1-294} (Fig. 3B) and in CHO-$GHR_{\Delta 297-311}$ (Fig. 3C). In the same way, no change in oxidized flavoproteins autofluorescence was detected in CHO-GHR_{1-638} cells in response to rGH (Figs. 5A and 6A).

The deletion of total GHR intracellular domain results in the impairment of signal transduction as shown in CHO-GHR_{1-294} cells characterized by the absence of the hormone endocytosis phenomenon (Fig. 7A). GH and GHR immunoreactivities did not present any variation following rGH stimulation. GH did not internalize in these cells, and the GHR distribution pattern was similar in control and in stimulated cells (Fig. 7B). Moreover, the polarographic analysis did not reveal any significant variation in the oxygen consumption when compared to the control (Fig. 1B). Similarly, NADH (Figs. 3B and 4B) and oxidized flavoproteins (Figs. 5B and 6B) autofluorescence were not modified in response to rGH stimulation whatever the hormone concentration used.

The Box 1 of the GHR is involved in mitochondrial respiratory chain functioning

In CHO-$GHR_{\Delta 297-311}$ cells, exhibiting the absence of signal transduction mediated by Jak2 [3,5,6], no change in oxidative capacity in response to rGH stimulation occurs (Fig. 1B). Interestingly, if no variation in NADH autofluorescence intensity was observed (Figs. 3C and 4C), the lack of Box-1-dependent signal transduction induced an increase in signal intensity (Figs. 5C and 6C). In fact, a significant increase in oxidized flavoproteins autofluorescence ($P < 0.05$) appeared at 5 min and persisted during 30 min of rGH treatment (50 and 200 nM) (Fig. 6C). The maximum intensity was reached after 15-min incubation with 200 nM rGH showing a 25% increase compared to the control ($P < 0.05$) (Fig. 6C).

According to the results obtained with two-photon excitation microscopic analysis, NADH autofluorescence signal appeared stronger in CHO-GHR_{1-638} cells than in CHO-GHR_{1-294} and CHO-$GHR_{\Delta 297-311}$ cells, without GH treatment (Fig. 3). After 30-min rGH stimulation, NADH fluorescence intensity resulting from CHO-GHR_{1-294} and CHO-$GHR_{\Delta 297-311}$ cells remained unchanged, while it was stimulated in CHO-GHR_{F346A} and decreased in CHO-GHR_{1-638} and CHO-GHR_{1-454} cell types. The absence of photobleaching in all cells exposed for 30 min in the absence of rGH strongly suggested that this result is not likely due to artifacts.

The role of the GHR C-terminal domain in internalization and cellular respiration processes

Earlier observations indicated that in spite of the presence of Box 1, CHO-GHR_{1-454} cells were unable to activate the transcription of some genes [5] and intracellular free Ca^{2+} oscillations [6] in response to rGH. This was associated to a kinetic of GH uptake closely related to those described for CHO-GHR_{1-638} [9]. The half C-terminal part truncation of the intracellular domain altered neither GH trafficking nor GHR distribution. However, CHO-GHR_{1-454} cells exposed to 50 nM rGH exhibited a significant GH immunoreactivity in cytoplasmic and nuclear compartments already after 5 min (Fig. 8A). Between 15 and 30 min, the nucleus was particularly immunoreactive, indicating important nuclear translocation of the hormone (Fig. 8A). The immunocytochemical signal for GHR following GH exposure was mainly located in the perinuclear area. However, a translocation to the nucleus was observed within 15 min and was correlated with the nuclear uptake of GH. The nuclear GHR immunoreactivity was transient and declined within 30 min. Dual detection showed similar location of both GH and GHR immunolabeling essentially in the perinuclear area (Fig. 8A), suggesting that only a portion of GH could be imported to the nucleus under a complexed form with its receptor. The time course of GH endocytosis and GHR rearrangements was also measured by quantitative analysis in CHO-GHR_{1-454} cells (Fig. 8B). In cytoplasmic and nuclear compartments, variations of GH and GHR associated-fluorescence intensities were similar to those observed on CSLM images, confirming the previous description of

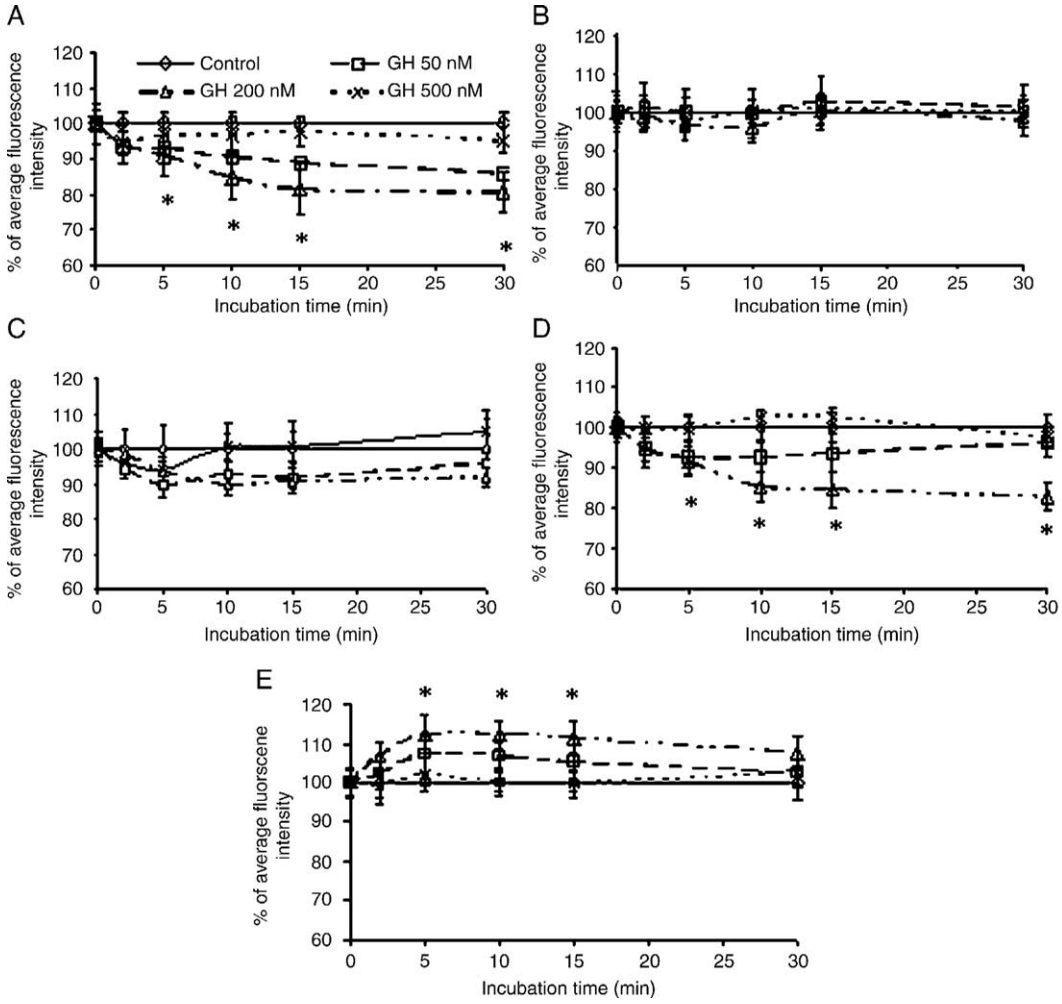

Fig. 4. Quantitative analysis of changes in NADH autofluorescence intensity in CHO cells expressing (A) the full-length GHR (CHO-GHR$_{1-638}$), (B) the GHR deleted of intracellular domain (CHO-GHR$_{1-294}$), (C) the GHR lacking the Box 1 region (CHO-GHR$_{\Delta 297-311}$),(D) the C-terminally truncated GHR (CHO-GHR$_{1-454}$) and (E) the GHR construct with a point mutation of phenylalanine 346 (CHO-GHR$_{F346A}$). The intrinsic fluorescence of NADH was quantified after 0, 2, 5, 10, 15 and 30 min of incubation with increasing GH concentrations of between 50 and 500 nM in each cell type as described in Materials and methods. Data are expressed as the mean of 3 experiments ± SEM. The results are normalized as a percentage of those obtained with the controls. The results were considered significant (*) at the 5% level.

changes in GH trafficking and GHR distribution [9]. GH immunoreactivity in both cellular compartments was early detectable (1 min) and reached a peak within 15 min (+75%) in cytoplasm and within 5 min in nucleus (+90%) (Fig. 8B). The GHR labeling variations displayed a cytoplasmic accumulation that remained quite stable from 1 to 30 min (the level stayed around +90/94%). This was associated to a nuclear translocation (+95%) as early as 1 min of GH treatment. Here, we observed an increase of GHR immunoreactivity in each cell compartment (+90%) until 15 min followed by a progressive decrease from 30 min on (not shown).

CHO-GHR$_{1-454}$ cells showed, like the CHO-GHR$_{1-638}$ cells, a significant activation of their respiration state ($P < 0.05$) (Fig. 1B). In both cases, oxygen consumption increased as early as 2 min following rGH stimulation and reached a maximum (about 50%) within 15 min but in a more attenuated manner in CHO-GHR$_{1-454}$ cells (Fig. 1B).

Similarly, after an exposure to 200 nM rGH during 30 min, CHO-GHR$_{1-454}$ cells presented a significant decrease in NADH signal intensity compared to 0 min time period ($P < 0.05$) (Fig. 4D). Moreover, no variation in FP autofluorescence was detected in these cells (Fig. 6D).

We then verified if internalization of GH and/or GHR could influence mitochondrial respiration by using confocal laser scanning microscopy, two-photon excitation fluorescence microscopy, transmission electron microscopy and biochemical approaches.

Regulation of cellular respiration by clathrin-coated pits internalization

Mutation of phenylalanine 346 residue in alanine resulted in serious alteration of GH internalization via clathrin pathway (Fig. 9A) confirming previously described

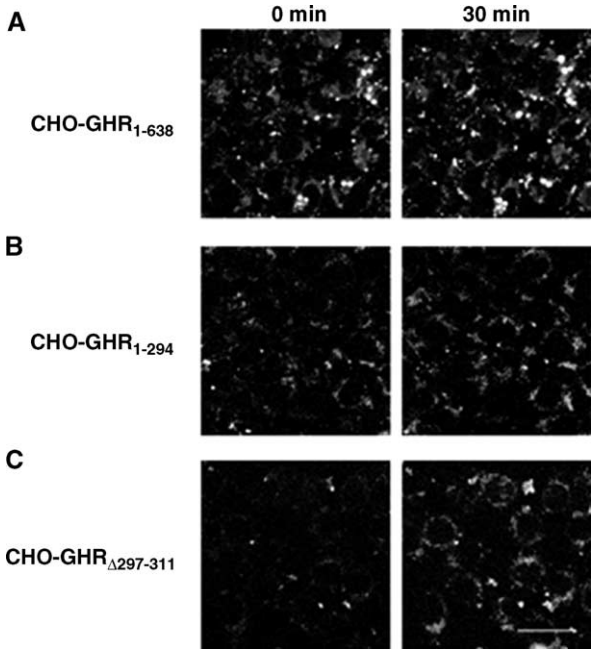

Fig. 5. Effect of 30-min exposure to 200 nM rGH on oxidized flavoproteins autofluorescence in CHO cells expressing (A) the full-length GHR (CHO-GHR_{1-638}), (B) the GHR deleted of intracellular domain (CHO-GHR_{1-294}) and (C) the GHR lacking the Box 1 region (CHO-$GHR_{\Delta 297-311}$). The intrinsic fluorescence of oxidized flavoproteins was visualized in the left hand column for the controls and in the right hand column for GH-stimulated CHO cells by one-photon excitation confocal laser scanning microscopy. Magnification bar is 30 μm for all photographs.

observations [13]. Although signal intensity remained very low, GH immunoreactivity was already detectable from 1 to 30 min in both the cytoplasm and the nucleus and was closely related to changes in GHR distribution (Fig. 9A). GHR immunolabeling distribution varied depending on whether cells were incubated with or without GH. A slight perinuclear accumulation and nuclear translocation of GHR occurred between 1 and 30 min. Dual detection of signal immunoreactivities for GH and GHR showed GH mainly localized in the nucleus and partly colocalized to its receptor. Quantitative analysis corroborated these results (Fig. 9B). The GH-associated signal reach a peak later (15 min) than in CHO-GHR_{1-638} cells were the maximum fluorescence intensity was collected. In the nucleus, the GH translocation was delayed compared to control. At the same time, GHR signal intensity increased by 15% in each subcellular compartment between 1 and 30 min. Based on these results, this mutation which prevented ubiquitin GHR conjugation could strongly delay GH internalization and nuclear translocation without inhibition. A decrease of oxygen consumption was observed in CHO-GHR_{F346A} cells (Fig. 1B). The respiratory activity dropped to the lowest level as early as 2 min after rGH exposure ($P < 0.05$) and tended towards control within 15 min. The mutation of phenylalanine 346 residue resulted in a transient increase in NADH signal intensity (10%) detectable from 2 min and statistically significant from 5 to 15 min ($P < 0.05$) with 50 and 200 nM rGH (Fig. 4E). Inversely, no modification of FP autofluorescence was detected (Fig. 6E).

Regulation of cellular respiration by caveolar internalization

Caveolin-1, GH and GHR were detected in control rat liver ultrathin frozen sections by immunogold electron microscopy. Colocalization of GH and caveolin-1, using 10- and 5-nm gold particles respectively, was observed in the Disse's space (not shown), in the cytosol and within mitochondria (Fig. 10A). GHR and caveolin-1 were also coimmunodetected near and within mitochondria (Fig. 10C). In control experiments, the specificity of the immunocytochemical reactions was assessed by omission of the primary antibodies (Fig. 10B). Moreover, we wanted to put caveolin-1 in evidence by a biochemical approach: Western blot analysis of rat liver and mitochondrial fractions showed a protein band between 20 kDa and 30 kDa (Fig. 11). It corresponds to caveolin-1 molecular weight (21–25 kDa) [17].

GH mitochondrial uptake has been shown in vivo using ^{125}I-GH [31] in rat liver, and GHR immunoreactivity was demonstrated in rat pituitary mitochondria [49]. By this study, we wanted to verify if, when isolated from the cytoplasmic environment, mitochondria could still present GH and GHR immunoreactivities.

Quantitative analysis of the immunocytochemical detection of GH, GHR and caveolin-1 on sections of fractions of isolated mitochondria embedded in LR-White resin showed that after a stimulation of 10 min with rGH, GH immunolabeling was significantly increased by 3.29 times comparing to control ($P < 0.05$) (Table 1). However, no change was observed for GHR and caveolin-1 labeling densities (Table 1).

When CHO-GHR_{1-638} cells were treated with methyl-β-cyclodextrin in order to alter caveolae internalization by depleting membrane cholesterol, oxygen consumption in GH-stimulated cells was not different from control samples without GH incubation or from controls without drug and GH administration (Fig. 12).

Discussion

Our observations of GH effects taking place in mitochondria demonstrate the following points: first, the lack of total GHR intracellular domain cannot induce any internalization or signal transduction and consequently presents no effect on the cellular respiratory state. Second, internalization and signal transduction are independent events concerning their initiation: the cells expressing the GHR lacking the Box 1 region are unable to induce any signal transduction translating thus no effect on respiration through NADH oxidation but internalize normally the

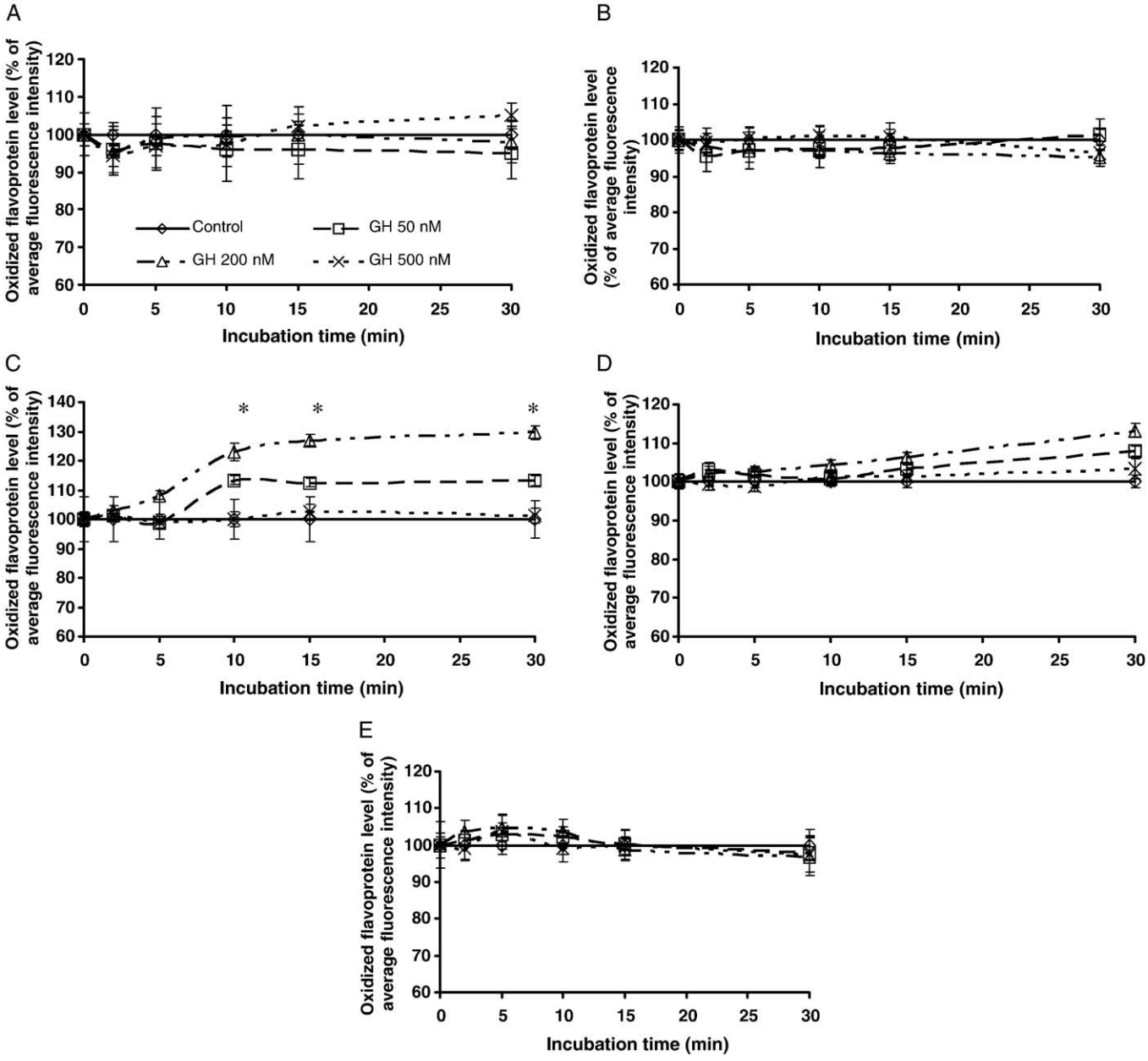

Fig. 6. Quantitative analysis of changes in oxidized flavoproteins autofluorescence intensity in CHO cells expressing (A) the full-length GHR (CHO-GHR_{1-638}), (B) the GHR deleted of intracellular domain (CHO-GHR_{1-294}), (C) the GHR lacking the Box 1 region (CHO-$GHR_{\Delta 297-311}$), (D) the C-terminally truncated GHR (CHO-GHR_{1-454}) and (E) the GHR construct with a point mutation of phenylalanine 346 (CHO-GHR_{F346A}). The intrinsic fluorescence of oxidized flavoproteins was quantified after 0, 2, 5, 10, 15 and 30 min of incubation with increasing GH concentrations of between 50 and 500 nM in each cell type as described in Materials and methods. Data are expressed as the mean of 3 experiments ± SEM. The results are normalized as a percentage of those obtained with the controls, which were taken to represent 100% of maximal oxygen consumption. The results were considered significant (*) at the 5% level.

GH-GHR_2 complex [9]. Third, the GHR C-terminal region (residues 455 to 638) seems to be involved only partially in respiration GH effect since its deletion influences weakly NADH oxidation and global respiration. Moreover, this deletion does not disrupt internalization, demonstrating that this domain is not related to endocytosis. Fourth, the UbE motif and caveolae are clearly involved in GH-GHR_2 internalization. The cells that expressed the GHR presenting the punctual mutation of the phenylalanine 346 residue and the cells where the formation of caveolae was impaired showed a perturbation in their respiratory state, suggesting the implication of the internalization phenomenon in the regulation of GH effects. Fifth, we detected in vivo and in vitro GH, GHR and caveolin-1 within mitochondria, proposing the involvement of the caveolae pathway in GH and GHR targeting to this organelle.

Previous investigations have studied GH subcellular localization in hypophysectomized or GH-deficient rats and have attempted to correlate GH mitochondrial

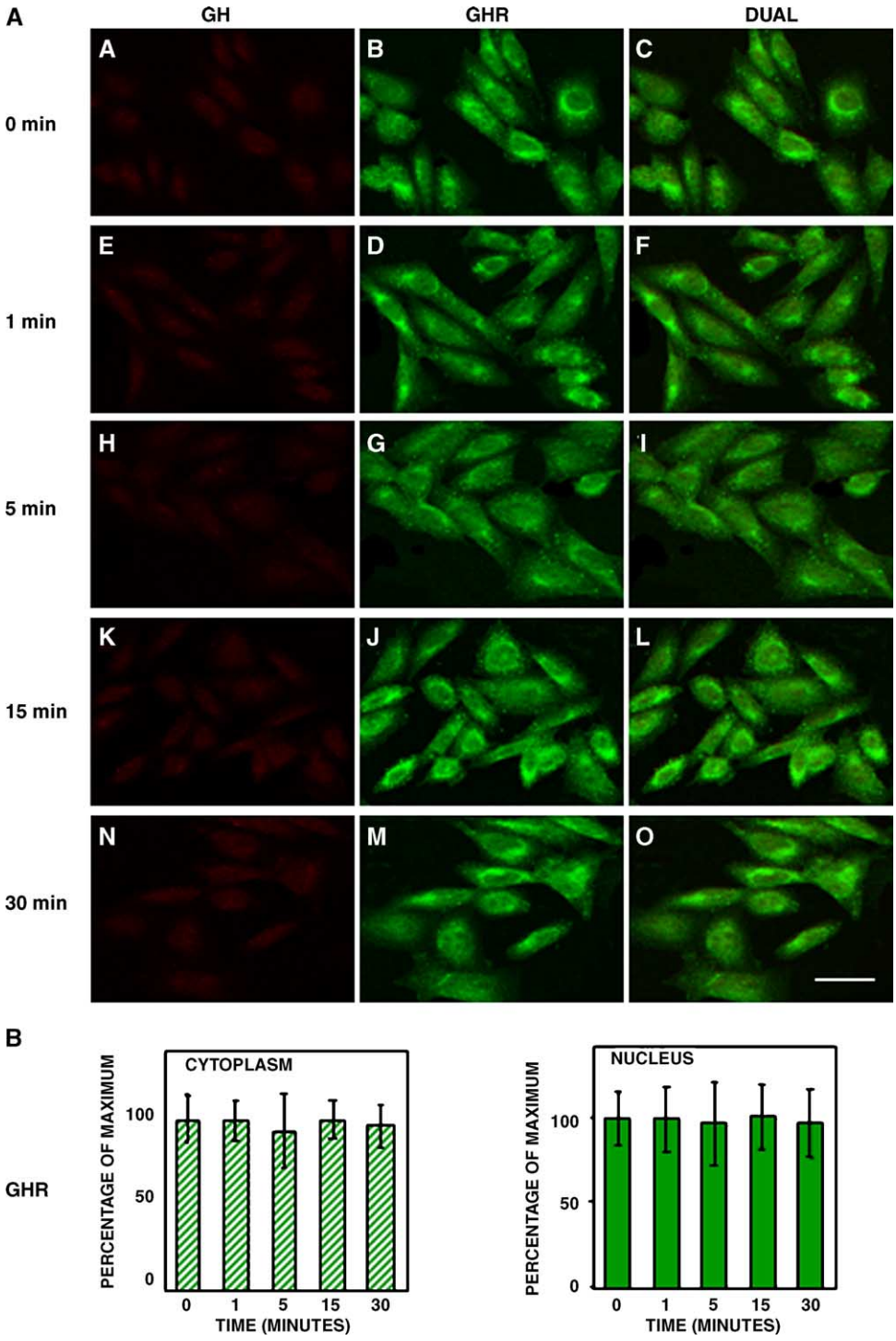

Fig. 7. (A) Kinetics of GH and GHR internalization and nuclear translocation in CHO cells expressing the GHR deleted of intracellular domain (CHO-GHR_{1-294}). Confocal laser scanning microscopy analysis was performed at 0, 2, 5, 15 and 30 min after 50 nM rGH stimulation as described in Materials and methods. The localization of GH is exposed in the left hand column, the GHR in the middle column and the dual localization (surimposed images) in the right hand column. (B) Quantitative analysis of GH and GHR internalization and nuclear translocation in CHO-GHR_{1-294} cells. GH and GHR immunoreactivities were quantified in cytoplasm and nucleus as described in Materials and methods. Data are expressed as the mean of normalized values from 3 experiments ± SEM and are considered significantly different from control at the 95% confidence level from 100% of maximal signal intensity. Magnification bar, 30 μm for all photographs.

localization with an oxidative dysfunction [31,32,50,51]. Reports have suggested a GH-induced regulation in the mitochondrial oxidative function of liver cells from GH-treated hypophysectomized rats [25–27,52], yet other studies have been unable to confirm any changes in hepatic mitochondrial respiration [28–30].

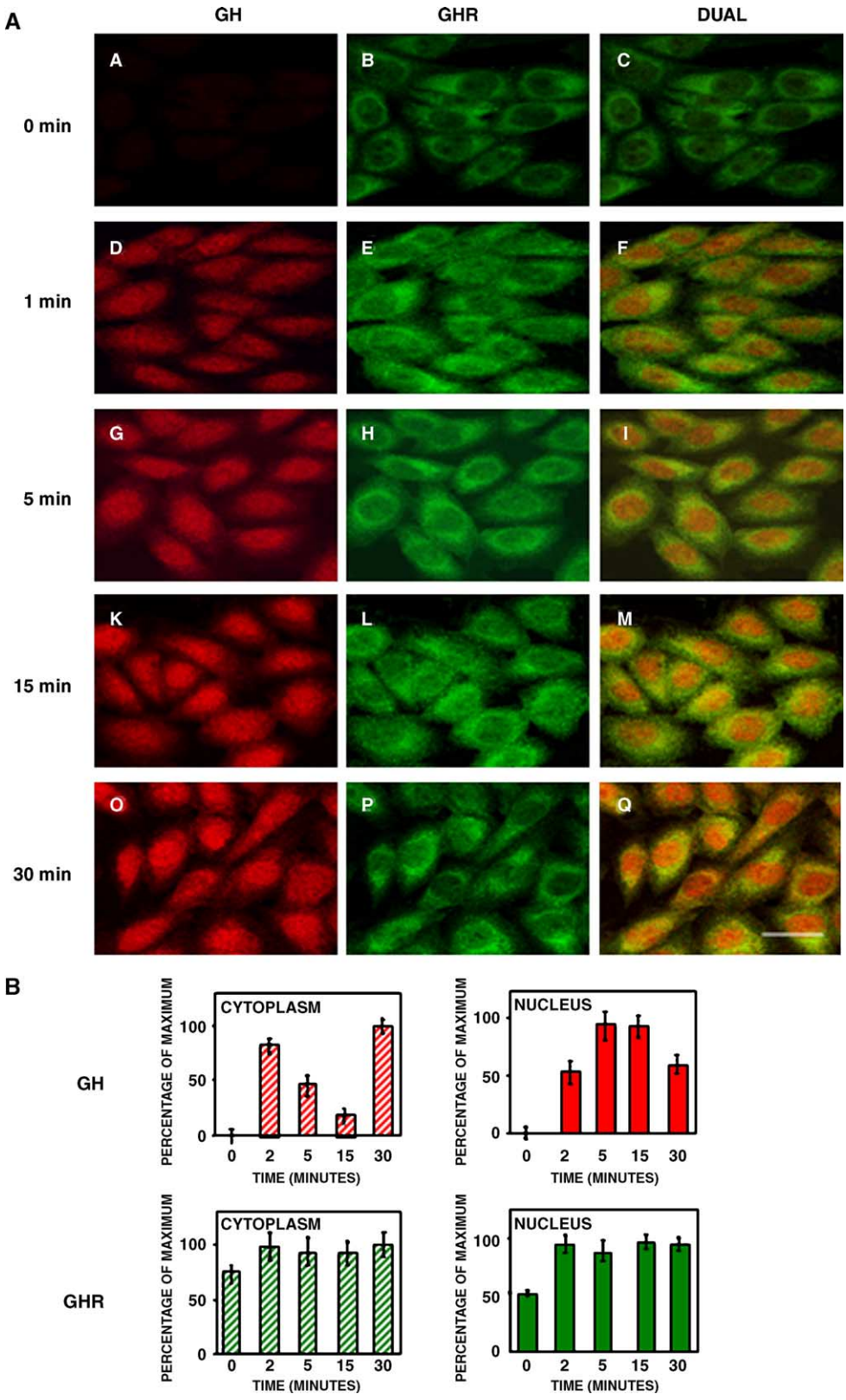

Fig. 8. (A) Kinetics of GH and GHR internalization and nuclear translocation in CHO cells expressing a C-terminally truncated GHR (CHO-GHR_{1-454}). Confocal laser scanning microscopy analysis was performed at 0, 2, 5, 15 and 30 min after 50 nM rGH stimulation as described in Materials and methods. The localization of GH is exposed in the left hand column, the GHR in the middle column and the dual localization (surimposed images) in the right hand column. (B) Quantitative analysis of GH and GHR internalization and nuclear translocation in CHO-GHR_{1-454} cells. GH and GHR immunoreactivities were quantified in cytoplasm and nucleus as described in Materials and methods. Data are expressed as the mean of normalized values from 3 experiments ± SEM and are considered significantly different from control at the 95% confidence level from 100% of maximal signal intensity. Magnification bar is 30 μm for all photographs.

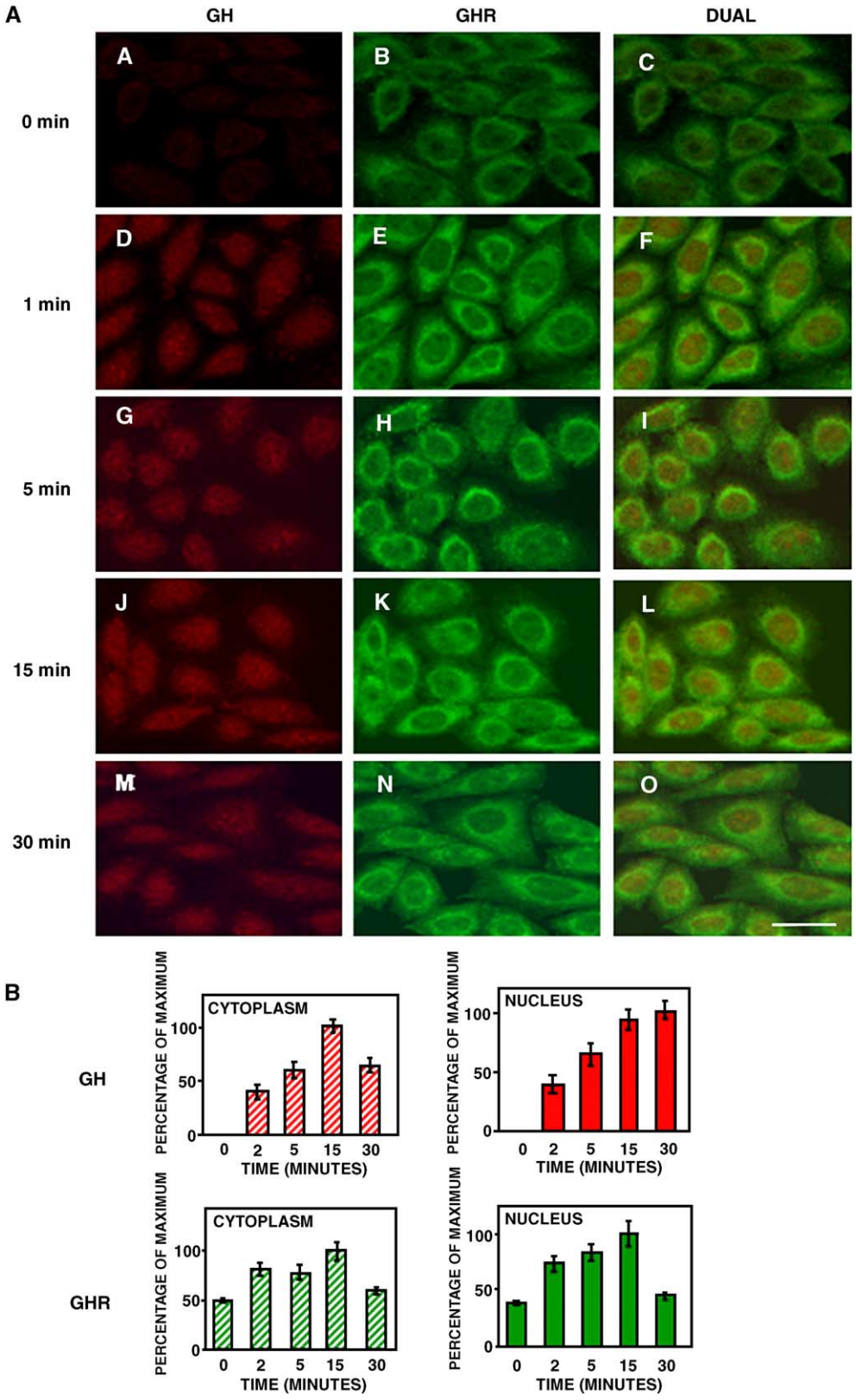

Fig. 9. (A) Kinetics of GH and GHR internalization and nuclear translocation in CHO cells expressing a GHR construct with a point mutation of phenylalanine 346 (CHO-GHR_{F346A}). CSLM analysis was performed at 0, 2, 5, 15 and 30 min after 50 nM rGH stimulation as described in Materials and methods. The localization of GH is exposed in the left hand column, the GHR in the middle column and the dual localization (surimposed images) in the right hand column. (B) Quantitative analysis of GH and GHR internalization and nuclear translocation in CHO-GHR_{F346A} cells. GH and GHR immunoreactivities were quantified in cytoplasm and nucleus as described in Materials and methods. Data are expressed as the mean of normalized values from 3 experiments ± SEM and are considered significantly different from control at the 95% confidence level from 100% of maximal signal intensity. Magnification bar, 30 μm for all photographs.

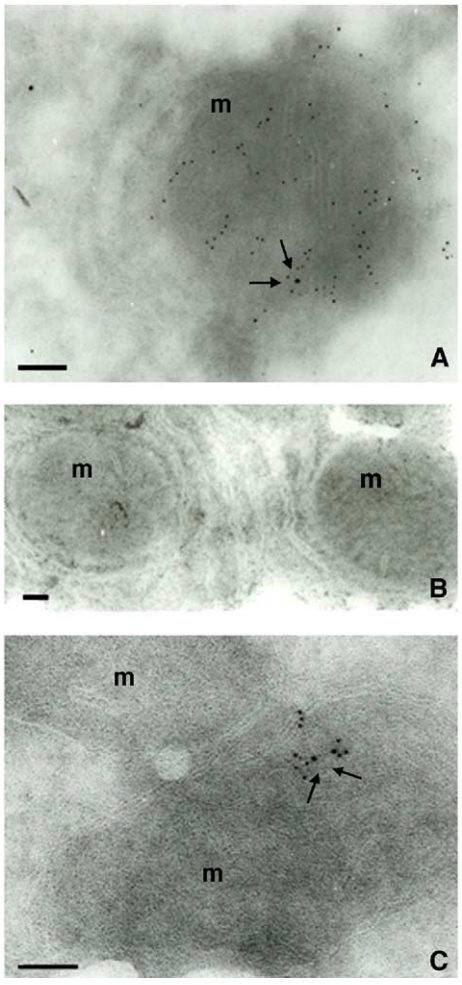

Fig. 10. (A) Double immunodetection of caveolin-1 and GH on control rat liver ultrathin frozen sections. GH (10-nm gold particles) and caveolin-1 (5-nm gold particles) were colocalized in the cytoplasmic compartment and within mitochondria. (B) Control without primary antibody presented no signal. (C) Double immunodetection of caveolin-1 and GHR on rat liver ultrathin frozen sections. GHR (10-nm gold particles) was colocalized with caveolin-1 (5-nm gold particles) within mitochondria (arrows). m: mitochondrion. Scale bar represents 100 nm.

In order to determine the ways by which GH could regulate the mitochondrial respiration through the interaction with its specific receptor, we have examined the ability

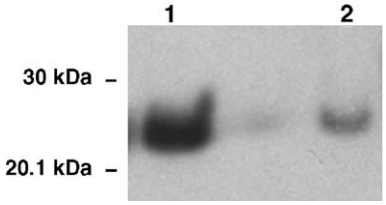

Fig. 11. Characterization of caveolin-1 in mitochondria. SDS-polyacrylamide gel electrophoresis was performed on liver and mitochondrial fractions obtained as described in Materials and methods from control rat. Caveolin-1 was detected in rat liver fraction containing 30 μg protein (lane 1) and in isolated rat mitochondria samples comprising 30 μg protein (lane 2). The band was found at the molecular weigh between 20 and 30 kDa, corresponding to the caveolin-1 known molecular weigh (22–25 kDa).

Table 1
Quantitative evaluation of electron microscopic immunodetection of GH, GHR and caveolin-1 in isolated mitochondria embedded in LR-White resin

	Control	GH stimulated
Anti-GH	1.36 ± 0.17	4.48 ± 0.68*
Anti-GHR	1.55 ± 0.05	3.13 ± 0.92
Anti-caveolin-1	4.8 ± 0.68	4.33 ± 1.06

The data in the table represent the labeling density mean (number of gold particles per square micrometer ± SE). After the GH stimulation, GH immunolabeling was significantly increased by about 3 times comparing to control. The level of anti-caveolin-1 and anti-GHR signals remained stable in both control and GH stimulated cells. Results were considered significant at the 5% level.
Control: sample of mitochondria that were not incubated in presence of GH.
GH stimulated: sample of mitochondria that were stimulated during 10 min with 50 nM GH.
* $P < 0.05$.

of mutated and truncated GHRs to generate variation in NADH and oxidized flavoproteins autofluorescence in rGH short-term exposed CHO cells. Two-photon excitation microscopy was used to visualize these signals and the interpretation of the variations of the autofluorescence is that a decrease in NADH fluorescence expressed an increase in NADH-oxidized form which could result from an acceleration of respiratory chain activity or from a slow-down in NADH formation. In the same way, an increase in FAD fluorescence could result from an acceleration of

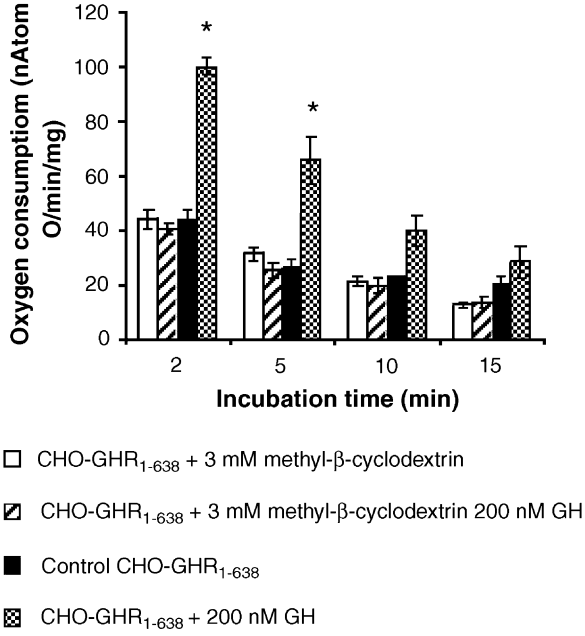

Fig. 12. Polarographic analysis of CHO cells expressing the full-length GHR (CHO-GHR_{1-638}) in response to 200 nM rGH stimulation. Oxygen consumption was analyzed as described in Materials and methods. Cells underwent or not a 3 mM methyl-β-cyclodextrin incubation for 1 h at 37°C and then were stimulated or not with 200 nM rGH. Control corresponds to polarographic analysis performed on CHO-GHR_{1-638} without GH incubation. The results are expressed in nAtom of oxygen per minute per milligram of protein, as the mean of 5 experiments ± SEM. Results were considered significant at the 5% level.

mitochondrial respiration or from an increase in oxidized flavoproteins amount covalently bound to FAD in mitochondria [53]. It has long been admitted that NADH and FAD act simultaneously in response to stimuli suggesting their colocalization in a same compartment. Strikingly, observation of NADH and FAD autofluorescence codetection revealed that the 2 cofactors are not always expressed at the same time in the same mitochondrion. Intracellular functional heterogeneity of mitochondria has been demonstrated for several cell types, suggesting that various mitochondrial subpopulations may be differently involved in physiologic and pathologic processes [54,55]. It was shown that the efficiency of oxidative phosphorylations depended on the nature of the respiratory substrates, which feed the respiratory chain on electrons at different levels (reviewed by [56]). Moreover, it has already been proposed that cells could display a wide range of mitochondrial morphologies as well as heterogeneous mitochondrial functionalities, raising the possibility that subpopulations of these organelles could carry out diverse processes within different areas of a cell [57]. The distribution of the 2 cofactors we observed in the present work (Fig. 2) suggests 2 different interpretations: either there are 2 distinct mitochondrial subpopulations using selectively NADH or FAD; or a given mitochondrion uses preferentially one of the 2 cofactors according to its physiological need. Indeed, it was previously suggested [58] that hepatocytes could tolerate very different respiratory capacities according to cellular energy demand.

To evaluate the respiratory state corresponding to NADH and FAD variation, we performed a cell respiration analysis using polarography. In parallel, to determine the part played by the receptor in the variations of cofactor autofluorescence, we studied the response to GH exposure of CHO cells expressing deleted or mutated GHRs. The use of GHR deleted of its intracellular domain (GHR_{1-294}) expressed in CHO cells made it possible to demonstrate the GHR implication in GH-stimulated cellular respiration. In agreement with previous studies which showed the role of GHR Box 1 in signal transduction [2–6], the lack of intracellular domain does not induce any GH effect on oxygen consumption or NADH and oxidized flavoproteins fluorescence.

Using CHO cells expressing the full-length GHR (GHR_{1-638}) and the C-terminally truncated GHR (GHR_{1-454}), we observed a decrease in NADH autofluorescence as early as 2 min upon GH stimulation, while no change in FAD autofluorescence occurred. Simultaneously, respiratory response to GH administration of these cells was rapidly increased. However, in CHO cells stably transfected with the Box 1 deleted GHR cDNA ($GHR_{\Delta 297-311}$), no variation has been detected neither in NADH autofluorescence nor in oxidative capacity. Only the oxidized flavoprotein fluorescence increased in response to GH. These results likely indicate the Box 1 involvement in GH-stimulated cellular respiration mediated by NADH oxidation. The CHO-$GHR_{\Delta 297-311}$ cells constituted the only cell type to show specific oxidized flavoproteins autofluorescence increase, reinforcing the hypothesis that NADH and FAD could be differentially distributed according to their assigned role.

We postulated that GH could induce a stimulation of mitochondrial respiration resulting from GHR-dependent intracellular signaling and/or GH internalization. In order to elucidate the underlying mechanism, we needed to understand the role played by the receptor in the GH endocytic machinery. By studying CHO cells expressing the GHR construct deleted of intracellular domain (CHO-GHR_{1-294}), we observed an absence of GH internalization and GHR rearrangements, confirming the functional importance of GHR cytoplasmic region in GH endocytosis. The presence of GH internalization in CHO-$GHR_{\Delta 297-311}$ cells revealed, in agreement with previous observations [9], that neither deletion in Box 1 nor Box 1 prolines mutation changed the kinetics of GH internalization, even when the nuclear retention of the hormone was increased. The critical role for phenylalanine 346 residue [13] was also verified by the demonstration of a weaker internalization efficiency of the hormone and GHR down-regulation in CHO-GHR_{F346A} cells. As described by Govers et al. [12], the GH/GHR complex was internalized in an ubiquitin-dependent manner by a way involving a DSWVEFIELD domain of the receptor (the UbE motif) in which the phenylalanine residue at position 346 was critical [13]. The UbE motif was required for efficient incorporation of GHR in clathrin-coated pits [59], so it was likely that mutation of phenylalanine 346 residue in alanine (GHR_{F346A}) disrupted the GHR clathrin-mediated endocytosis. A role for caveolae in GH internalization has been suggested by Lobie et al. [8]. Thus, we supposed that the detection of remaining GH immunoreactivity observed during 30 min after GH exposure in CHO-GHR_{F346A} could result from this endocytic pathway. Caveolae present different functions according to their lipid and protein composition favoring many different roles dictated by the actual demand of the cell, for example, the stage of growth, differentiation or transformation. These structures are well known for their implication in processes such as intracellular signaling [18–20], tumor progression [60] and lipid [61] and protein transport [8,62]. It is now well established that the complex GH-GHR_2 is internalized in cells via the clathrin-coated pits route [10], but a study demonstrated GH-GHR_2 internalization via the caveolae pathway in CHO transfected cells [8]. For interferon γ (IFNγ), member of the same cytokine superfamily as GH, two pathways were proposed: one directed by clathrin-coated pits which was supposed to target the hormone-receptor complex to lysosomal fraction and degradation [7], and one orchestrated by caveolae vesicles should drive IFNγ to other intracellular compartments [48,63]. Now, recent data [64] suggest that the clathrin coat is involved in lysosomal-targeted GHR, reinforcing the idea that the clathrin-coated

pits target the complex to the degradation pathway and that the caveolae route would be used for the intracellular transport of GH. Moreover, these two internalization pathways were shown to take part in TGF-β signaling and turnover [62,65].

We therefore decided to study GH caveolar internalization by means of immunoelectron microscopy in liver, the main GH target tissue, rich in mitochondria. GH uptake has been investigated in rat liver at the beginning of the 70s by Groves, Maddaiah, and collaborators [25,51,66]. They reported that GH was implicated in the regulation of mitochondrial biogenesis in liver tissue through a direct interaction of the hormone with mitochondrial membranes [50,51]. However, some later studies were conflicting with these data. Postel-Vinay et al. [28], analyzing subcellular distribution of [^{125}I]-hGH iv injected to female rats, demonstrated that hGH was internalized in vivo in the hepatocyte, but virtually no radioactivity was associated with mitochondria. This observation was corroborated by another report [29], focusing on T_3 and GH action on mitochondrial biogenesis and concluding that only T_3 had an effect whereas no high affinity binding sites for GH were present in rat liver mitochondria. Moreover, specific binding sites for [^{125}I]-T_3 after injection, as well as T_3 receptor-like immunoreactivity were revealed in rat liver mitochondria [67]. The presence of another receptor belonging to the steroid-thyroid receptor superfamily, the glucocorticoid receptor, was reported to localize within mitochondria of human cells [68], suggesting the direct action of glucocorticoids on mitochondrial metabolism. In the present study, we clearly show that GH induced an increase in oxygen consumption in CHO cells expressing the full-length GHR. This finding indicates a real effect of GH on mitochondrial function as it was proposed for thyroid hormones [69]. Moreover, here, we show GH and GHR binding to mitochondrial membranes, but the resolution does not allow us to decide which of the 2 membranes (inner or outer) are involved. Actually, liver does not express GH mRNA but represents a major GH target tissue. This accounts for a high GHR immunoreactivity observed in our experiments, reflecting flow of GH provided by blood circulation.

Caveolin-1 is selectively associated to lipid rafts, forming caveolae and appears to be the major protein of the caveolin family in many cell types [17]. Caveolin-1 has been identified in liver subcellular fractions [70,71] and also in mitochondria [72]. We therefore hypothesized about a possible role of caveolae in mitochondrial import. Immunoelectron microscopy on rat liver ultrathin frozen sections allowed us to colocalize caveolin-1 with either GH or GHR in the same cellular compartments. As caveolin-1 was previously detected in blood vessel endothelium [73], caveolae may therefore play a transcytosis role allowing GH to enter the hepatic cell. Our quantitative evaluation of anti-GH, anti-GHR and anti-caveolin-1 immunogold labeling performed on isolated mitochondria demonstrated that after GH stimulation, only GH mitochondrial immunolabeling was significantly increased ($P < 0.05$), contrary to caveolin-1 and GHR labeling that remained stable. These findings suggest the preexistence of the receptor and caveolin-1 within mitochondria.

When the pathway of caveolae, in CHO-GHR_{1-638} cells, and of the clathrin-coated pits in GHR_{F346A} cells, were disrupted, GH could no more exert its stimulatory effect on oxygen consumption. Caveolin-1 is known to interact with signaling molecules [18–20] and was particularly supposed to be part of a structure (caveolae) assimilated to a potential platform for GH signaling [74]. In this way, if the complex GH/GHR is not internalized by caveolae, there is a lack in the signaling transduction. Inversely, in CHO-GHR_{F346A} cells, the increase in NADH fluorescence associated to the lack of FAD fluorescence variation and concomitantly to an inhibition of metabolic response to GH suggests the existence of a negative regulatory mechanism dependent on GHR involving NAD reduction. One could then speculate about a possible interaction between the signal transduction and the internalization pathways resulting in the regulation of GH action.

It is now admitted that the GHR C-terminal domain is responsible for gene transcription [5] and intracellular free Ca^{2+} oscillations [6]. However, our data demonstrate that the cells expressing the GHR lacking the c-terminal domain can have the same stimulatory effect on mitochondrial function as the full-length receptor. We already knew that Jak2 activity and/or tyrosine phosphorylation within the cell is not required for internalization and nuclear translocation of the hormone [9]. Thus, we confirmed that GH endocytosis was independent of GHR molecular domains integrity responsible for intracellular signaling.

In conclusion, we have demonstrated that GH stimulates cellular oxygen consumption through GHR signaling pathway involving Box 1 region via NADH oxidation. This resulting effect includes a direct GH stimulation of respiration and a regulation mechanism according to the pathway used by the cell to internalize the hormone. We showed that GH and GHR were internalized to the mitochondria through a new pathway constituted by caveolea. In this way, when the hormone is not endocytosed by the caveolae or the clathrin-coated pits route, the GH effect on mitochondrial function is impaired.

Acknowledgments

The authors are grateful to Dr. M.J. Waters (Queensland University, Brisbane) for providing murine anti-rGHR. They also want to thank Dr. S. Fakan for critical reading of the manuscript and for helpful comments. This work was supported in part by a grant from La Région Rhône-Alpes, Emergence 2002.

References

[1] J. Finidori, P.A. Kelly, Cytokine receptor signalling through two novel families of transducer molecules: Janus kinases, and signal transducers and activators of transcription, J. Endocrinol. 147 (1995) 11–23.

[2] J.A. Vanderkuur, X. Wang, L. Zhang, G.S. Cambell, G. Allevato, N. Billestrup, G. Norstedt, C. Carter-Su, Domains of the growth hormone receptor required for association and activation of JAK2 tyrosine kinase, J. Biol. Chem. 269 (1994) 21709–21717.

[3] C. Carter-Su, L.S. Smit, Signaling via JAK tyrosine kinases: growth hormone receptor as a model system, Recent Prog. Horm. Res. 53 (1998) 61–83.

[4] L. Goujon, G. Allevato, G. Simonin, L. Paquereau, A. Le Cam, J. Clark, J.H. Nielsen, J. Djiane, M.C. Postel-Vinay, M. Edery, P.A. Kelly, Cytoplasmic sequences of the growth hormone receptor necessary for signal transduction, Proc. Natl. Acad. Sci. U. S. A. 91 (1994) 957–961.

[5] A. Sotiropoulos, S. Moutoussamy, F. Renaudie, M. Clauss, C. Kayser, F. Gouilleux, P.A. Kelly, J. Finidori, Differential activation of Stat3 and Stat5 by distinct regions of the growth hormone receptor, Mol. Endocrinol. 10 (1996) 998–1009.

[6] N. Billestrup, P. Bouchelouche, G. Allevato, M. Ilondo, J.H. Nielsen, Growth hormone receptor C-terminal domains required for growth hormone-induced intracellular free Ca^{2+} oscillations and gene transcription, Proc. Natl. Acad. Sci. U. S. A. 92 (1995) 2725–2729.

[7] P. Roupas, A.C. Herington, Cellular mechanisms in the processing of growth hormone and its receptor, Mol. Cell. Endocrinol. 61 (1989) 1–12.

[8] P.E. Lobie, R. Sadir, R. Graichen, H.C. Mertani, G. Morel, Caveolar internalization of growth hormone, Exp. Cell. Res. 246 (1999) 47–55.

[9] H.C. Mertani, M. Raccurt, A. Abbate, J. Kindblom, J. Tornell, N. Billestrup, Y. Usson, G. Morel, P.E. Lobie, Nuclear translocation and retention of growth hormone, Endocrinology 144 (2003) 3182–3195.

[10] P. van Kerkhof, M. Sachse, J. Klumperman, G.J. Strous, Growth hormone receptor ubiquitination coincides with recruitment to clathrin-coated membrane domains, J. Biol. Chem. 276 (2001) 3778–3784.

[11] P. van Kerkhof, M. Smeets, G.J. Strous, The ubiquitin-proteasome pathway regulates the availability of the GH receptor, Endocrinology 143 (2002) 1243–1252.

[12] R. Govers, T. ten Broeke, P. van Kerkhof, A.L. Schwartz, G.J. Strous, Identification of a novel ubiquitin conjugation motif, required for ligand-induced internalization of the growth hormone receptor, EMBO. J. 18 (1999) 28–36.

[13] G. Allevato, N. Billestrup, L. Goujon, E.D. Galsgaard, G. Norstedt, M.C. Postel-Vinay, P.A. Kelly, J.H. Nielsen, Identification of phenylalanine 346 in the rat growth hormone receptor as being critical for ligand-mediated internalization and down-regulation, J. Biol. Chem. 270 (1995) 17210–17214.

[14] C.M. Alves dos Santos, T. ten Broeke, G.J. Strous, Growth hormone receptor ubiquitination, endocytosis, and degradation are independent of signal transduction via Janus kinase 2, J. Biol. Chem. 276 (2001) 32635–32641.

[15] K. Simons, D. Toomre, Lipid rafts and signal transduction, Nat. Rev., Mol. Cell. Biol. 1 (2000) 31–39.

[16] K. Simons, E. Ikonen, Functional rafts in cell membranes, Nature 387 (1997) 569–572.

[17] K.G. Rothberg, J.E. Heuser, W.C. Donzell, Y.S. Ying, J.R. Glenney, R.G. Anderson, Caveolin, a protein component of caveolae membrane coats, Cell 68 (1992) 673–682.

[18] T. Okamoto, A. Schlegel, P.E. Scherer, M.P. Lisanti, Caveolins, a family of scaffolding proteins for organizing "preassembled signaling complexes" at the plasma membrane, J. Biol. Chem. 273 (1998) 5419–5422.

[19] Y. Fujita, S. Maruyama, H. Kogo, S. Matsuo, T. Fujimoto, Caveolin-1 in mesangial cells suppresses MAP kinase activation and cell proliferation induced by bFGF and PDGF, Kidney Int. 66 (2004) 1794–1804.

[20] A. D'Alessio, R.S. Al-Lamki, J.R. Bradley, J.S. Pober, Caveolae participate in tumor necrosis factor receptor 1 signaling and internalization in a human endothelial cell line, Am. J. Pathol. 166 (2005) 1273–1282.

[21] P.H. Henneman, The effect of human growth hormone on growth of patients with hypopituitarism. A combined study, JAMA 205 (1968) 828–836.

[22] O.G. Isaksson, J.O. Jansson, I.A. Gause, Growth hormone stimulates longitudinal bone growth directly, Science 216 (1982) 1237–1239.

[23] M.B. Davidson, Effect of growth hormone on carbohydrate and lipid metabolism, Endocr. Rev. 8 (1987) 115–131.

[24] G.A. Dudley, R. Portanova, Histochemical characteristics of soleus muscle in hGH transgenic mice, Proc. Soc. Exp. Biol. Med. 185 (1987) 403–408.

[25] D.M. Katkocin, K.M. Gupta, P.J. Collipp, V.T. Maddaiah, Effects of growth hormone on respiration and ATPase activity of rat liver and heart mitochondria, Biochem. Med. 22 (1979) 134–144.

[26] S. Clejan, P.J. Collipp, V.T. Maddaiah, Hormones and liver mitochondria: influence of growth hormone, thyroxine, testosterone, and insulin on thermotropic effects of respiration and fatty acid composition of membranes, Arch. Biochem. Biophys. 203 (1980) 744–752.

[27] V.T. Maddaiah, S. Clejan, Growth hormone and liver mitochondria: time course of effects on respiration and fatty acid composition in hypophysectomized rats, Endocrinology 119 (1986) 250–252.

[28] M.C. Postel-Vinay, C. Kayser, B. Desbuquois, Fate of injected human growth hormone in the female rat liver in vivo, Endocrinology 111 (1982) 244–251.

[29] A. Mutvei, B. Husman, G. Andersson, B.D. Nelson, Thyroid hormone and not growth hormone is the principle regulator of mammalian mitochondrial biogenesis, Acta Endocrinol. (Copenh.) 121 (1989) 223–228.

[30] C. Peyreigne, E. Raynaud, C. Fedou, C. Prefaut, J.F. Brun, J. Mercier, Does growth hormone treatment alter skeletal muscle mitochondrial respiration in rats? Horm. Res. 58 (2002) 287–291.

[31] P.E. Lobie, H. Mertani, G. Morel, O. Morales-Bustos, G. Norstedt, M.J. Waters, Receptor-mediated nuclear translocation of growth hormone, J. Biol. Chem. 269 (1994) 21330–21339.

[32] H.C. Mertani, M.J. Waters, G. Morel, Cellular trafficking of exogenous growth hormone in dwarf rat pituitary, Neuroendocrinology 63 (1996) 257–268.

[33] N. Billestrup, A. Møldrup, P. Serup, L.S. Mathews, G. Norstedt, J.H. Nielsen, Introduction of exogenous growth hormone receptors augments growth hormone-responsive insulin biosynthesis in rat insulinoma cells, Proc. Natl. Acad. Sci. U. S. A. 87 (1990) 7210–7214.

[34] A. Møldrup, G. Allevato, T. Dyrberg, J.H. Nielsen, N. Billestrup, Growth hormone action in rat insulinoma cells expressing truncated growth hormone receptors, J. Biol. Chem. 266 (1991) 17441–17445.

[35] C. Möller, A. Hansson, B. Enberg, P.E. Lobie, G. Norstedt, Growth hormone (GH) induction of tyrosine phosphorylation and activation of mitogen-activated protein kinases in cells transfected with rat GH receptor cDNA, J. Biol. Chem. 267 (1992) 23403–23408.

[36] G. Villani, G. Attardi, In vivo control of respiration by cytochrome *c* oxidase in wild-type and mitochondrial DNA mutation-carrying human cells, Proc. Natl. Acad. Sci. U. S. A. 94 (1997) 1166–1171.

[37] R.S. Balaban, L.J. Mandel, Optical methods for the study of metabolism in intact cells, in: J.K. Foskett, S. Grinstein (Eds.), Non invasive Techniques in Cell Biology, Wiley-Liss, New York, 1990, pp. 213–236.

[38] B. Chance, Optical method, Annu. Rev. Biophys. Chem. 20 (1991) 1–28.

[39] B.R. Masters, B. Chance, Redox confocal imaging: intrinsic fluorescent probes of cellular metabolism, in: W.T. Mason (Ed.), Fluorescent and Luminescent Probes for Biological Activity, Academic Press, New York, 1993, pp. 44–57.

[40] V.A. Saks, V.I. Veksler, A.V. Kuznetsov, L. Kay, P. Sikk, T. Tiivel, L.

Tranqui, J. Olivares, K. Winkler, F. Wiedemann, W.S. Kunz, Permeabilized cell and skinned fiber techniques in studies of mitochondrial function in vivo, Mol. Cell. Biochem. 184 (1998) 81–100.
[41] W. Denk, J.H. Strickler, W.W. Webb, Two-photon laser scanning fluorescence microscopy, Science 248 (1990) 73–76.
[42] W. Denk, D.W. Piston, W.W. Webb, Two-photon molecular excitation in laser-scanning microscopy, in: J.B. Pawley (Ed.), Handbook of Biological Confocal Microscopy, Plenum Publishing, New York, 1995, pp. 445–458.
[43] C. Xu, W.W. Webb, Multiphoton excitation of molecular fluorophores and non-linear laser microscopy, in: J.R. Lakowics (Ed.), Topics in fluorescence Spectroscopy, vol. 5, Plenum Press, New York, 1997, pp. 471–540.
[44] Y. Usson, The two-photon microscope, in: X. Ronot, Y. Usson (Eds.), Imaging of Nucleic Acids and Quantitation in Photonic Microscopy, CRC-Press, 2001, pp. 80–84.
[45] D. Ardail, F. Gasnier, F. Lerme, C. Simonot, P. Louisot, O. Gateau-Roesch, Involvement of mitochondrial contact sites in the subcellular compartmentalization of phospholipid biosynthetic enzymes, J. Biol. Chem. 268 (1993) 25985–25992.
[46] J.E. Vance, Phospholipid synthesis in a membrane fraction associated with mitochondria, J. Biol. Chem. 265 (1990) 7248–7256.
[47] G. Morel, D. Gourdji, D. Grouselle, N. Brunet, A. Tixier-Vidal, P.M. Dubois, Immunocytochemical evidence for in vivo internalization of thyroliberin into rat pituitary target cells, Neuroendocrinology 41 (1985) 312–320.
[48] R. Sadir, A. Lambert, H. Lortat-Jacob, G. Morel, Caveolae and clathrin-coated vesicles: two possible internalization pathways for IFN-gamma and IFN-gamma receptor, Cytokine 14 (2001) 19–26.
[49] H.C. Mertani, M.J. Waters, R. Jambou, F. Gossard, G. Morel, Growth hormone receptor binding protein in rat anterior pituitary, Neuroendocrinology 59 (1994) 483–494.
[50] V.T. Maddaiah, I. Rezvani, S.Y. Chen, P.J. Collipp, Distribution of 3 H-acetyl human growth hormone in subcellular fractions of rat liver, Biochem. Med. 4 (1970) 492–499.
[51] W.E. Groves, G.E. Houts, G.S. Bayse, Subcellular distribution of 125 I-labeled bovine growth hormone in rat liver and kidney, Biochim. Biophys. Acta 264 (1972) 472–480.
[52] V.T. Maddaiah, S. Clejan, A.G. Palekar, P.J. Collipp, Hormones and liver mitochondria: effects of growth hormone and thyroxine on respiration, fluorescence of 1-anilino-8-naphthalene sulfonate and enzyme activities of complex I and II of submitochondrial particles, Arch. Biochem. Biophys. 210 (1981) 666–677.
[53] S. Huang, A.A. Heikal, W.W. Webb, Two-photon fluorescence spectroscopy and microscopy of NAD(P)H and flavoprotein, Biophys. J. 82 (2002) 2811–2825.
[54] T.J. Collins, M.J. Berridge, P. Lipp, M.D. Bootman, Mitochondria are morphologically and functionally heterogeneous within cells, EMBO J. 21 (2002) 1616–1627.
[55] A.V. Kuznetsov, Y. Usson, X. Leverve, R. Margreiter, Subcellular heterogeneity of mitochondrial function and dysfunction: evidence obtained by confocal imaging, Mol. Cell. Biochem. 256–257 (2004) 359–365.
[56] X.M. Leverve, E. Fontaine, Role of substrates in the regulation of mitochondrial function in situ, IUBMB Life 52 (2001) 221–229.
[57] T.J. Collins, M.D. Bootman, Mitochondria are morphologically heterogeneous within cells, J. Exp. Biol. 206 (2003) 1993–2000.
[58] V. Nogueira, M. Rigoulet, M.A. Piquet, A. Devin, E. Fontaine, X.M. Leverve, Mitochondrial respiratory chain adjustment to cellular energy demand, J. Biol. Chem. 276 (2001) 46104–46110.
[59] G.I. Strous, R. Govers, The ubiquitin-proteasome system and endocytosis, J. Cell. Sci. 112 (1999) 1417–1423.
[60] G. Fiucci, D. Ravid, R. Reich, M. Liscovitch, Caveolin-1 inhibits anchorage-independent growth, anoikis and invasiveness in MCF-7 human breast cancer cells, Oncogene 21 (2002) 2365–2375.
[61] C.J. Fielding, P.E. Fielding, Caveolae and intracellular trafficking of cholesterol, Adv. Drug Deliv. Rev. 49 (2001) 251–264.
[62] G.M. Di Guglielmo, C. Le Roy, A.F. Goodfellow, J.L. Wrana, Distinct endocytic pathways regulate TGF-beta receptor signalling and turnover, Nat. Cell. Biol. 5 (2003) 410–421.
[63] P.S. Subramaniam, H.M. Johnson, Lipid microdomains are required sites for the selective endocytosis and nuclear translocation of IFN-gamma, its receptor chain IFN-gamma receptor-1, and the phosphorylation and nuclear translocation of STAT1alpha, J. Immunol. 169 (2002) 1959–1969.
[64] M. Sachse, S. Urbe, V. Oorschot, G.J. Strous, J. Klumperman, Bilayered clathrin coats on endosomal vacuoles are involved in protein sorting toward lysosomes, Mol. Biol. Cell 13 (2002) 1313–1328.
[65] M. Felberbaum-Corti, F.G. Van Der Goot, J. Gruenberg, Sliding doors: clathrin-coated pits or caveolae? Nat. Cell Biol. 5 (2003) 382–384.
[66] V.T. Maddaiah, C.L. Weston, S.Y. Chen, P.J. Collipp, Growth hormone and liver mitochondria. Effects on cytochromes and some enzymes, Arch. Biochem. Biophys. 173 (1976) 225–230.
[67] D. Ardail, F. Lerme, J. Puymirat, G. Morel, Evidence for the presence of α and β-related T3 receptors in rat liver mitochondria, Eur. J. Cell Biol. 62 (1993) 105–113.
[68] K. Scheller, C.S. Sekeris, G. Krohne, R. Hock, I.A. Hansen, U. Scheer, Localization of glucocorticoid hormone receptors in mitochondria of human cells, Eur. J. Cell Biol. 79 (2000) 299–307.
[69] F. Goglia, E. Silvestri, A. Lanni, Thyroid hormones and mitochondria, Biosci. Rep. 22 (2002) 17–32.
[70] A. Pol, M. Calvo, C. Enrich, Isolated endosomes from quiescent rat liver contain the signal transduction machinery. Differential distribution of activated Raf-1 and Mek in the endocytic compartment, FEBS Lett. 441 (1998) 34–38.
[71] M. Calvo, C. Enrich, Biochemical analysis of a caveolae-enriched plasma membrane fraction from rat liver, Electrophoresis 21 (2000) 3386–3395.
[72] W.P. Li, P. Liu, B.K. Pilcher, R.G. Anderson, Cell-specific targeting of caveolin-1 to caveolae, secretory vesicles, cytoplasm or mitochondria, J. Cell Sci. 114 (2001) 1397–1408.
[73] S. Esser, K. Wolburg, H. Wolburg, G. Breier, T. Kurzchalia, W. Risau, Vascular endothelial growth factor induces endothelial fenestrations in vitro, J. Cell Biol. 140 (1998) 947–959.
[74] N. Yang, Y. Huang, J. Jiang, S.J. Frank, Caveolar and lipid raft localization of the growth hormone receptor and its signaling elements: impact on growth hormone signaling, J. Biol. Chem. 279 (2004) 20898–20905.